

Supporting Information

Probing the Local Structure of FLiBe Melts and Solidified Salt by in-situ High-temperature NMR

Xiaobin Fu^{1,3}, Yiyang Liu^{1,3}, Hailong Huang¹, Huiyan Wu^{1,2}, Jianchao Sun^{1,2}, Ling

Han^{1,2}, Min Ge¹, Yuan Qian^{1*}, Hongtao Liu^{1*}

¹ Department of Molten Salt Chemistry and Engineering, Shanghai Institute of Applied Physics, Chinese Academy of Sciences.

² University of Chinese Academy of Sciences, Beijing, 100049, China.

³ These authors contributed equally: Xiaobin Fu, Yiyang Liu

Corresponding Author

qianyuan@sinap.ac.cn;

liuhongtao@sinap.ac.cn;

Figure S1. ^9Be HT-NMR spectra of LiF-BeF₂ molten salts with different BeF₂ concentration.

Figure S2. Solid-state ^{19}F MAS NMR spectra and the signal intensity of FLiBe eutectic salts with different BeF₂ concentration.

Figure S3. XRD patterns of FLiBe eutectic salts with different BeF₂ concentration at room temperature.

Figure S4. Solid-state ^7Li MAS NMR spectra of FLiBe eutectic salts with different BeF₂ concentration.

Figure S5. Calculated LiF-BeF₂ phase diagram. (J. Mol. Liq. 299, 112165 (2020).)

Figure S6. Illustration of the laser-heating high-temperature NMR system.

Figure S7. High-temperature ^{19}F NMR signal simulations and the calculated average chemical shifts.

Figure S8. High-temperature ^9Be NMR signal simulations and the calculated average chemical shifts.

Figure S9. DFT calculation results of ^{19}F and ^9Be NMR chemical shifts of different Be-F species.

Figure S10. Calculated ^{19}F and ^9Be NMR chemical shift evolution plots.

Table S1. Simulated ^{19}F NMR signal chemical shifts.

Table S2. Simulated ^{19}F NMR signal integrals.

Table S3. Calculated ^{19}F NMR signal averaged chemical shifts.

Table S4. Simulated ^9Be NMR signal chemical shifts.

Table S5. Simulated ^9Be NMR signal integrals.

Table S6. Calculated ^9Be NMR signal averaged chemical shifts.

Figure S1. ^9Be HT-NMR spectra of LiF-BeF₂ molten salts with different BeF₂ concentration.

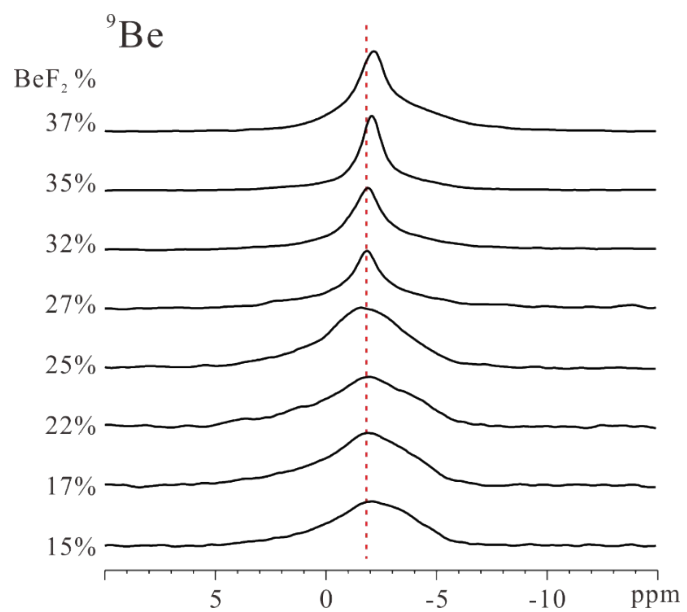
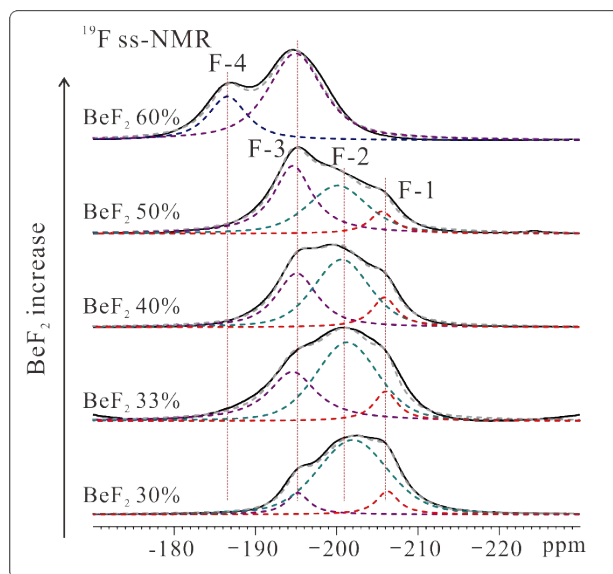


Figure S2. Solid-state ^{19}F MAS NMR spectra and the signal intensity of FLiBe eutectic salts with different BeF_2 concentration.



BeF_2 concentration	F-1	F-2	F-3	F-4
30%	10.5	79.5	9.9	0
33%	10.55	55.4	34.02	0
40%	13.07	51.92	35.01	0
50%	10.06	42.72	47.22	0
60%	0	0	72.9	27.1

Figure S3. XRD patterns of FLiBe eutectic salts with different BeF_2 concentration at room temperature.

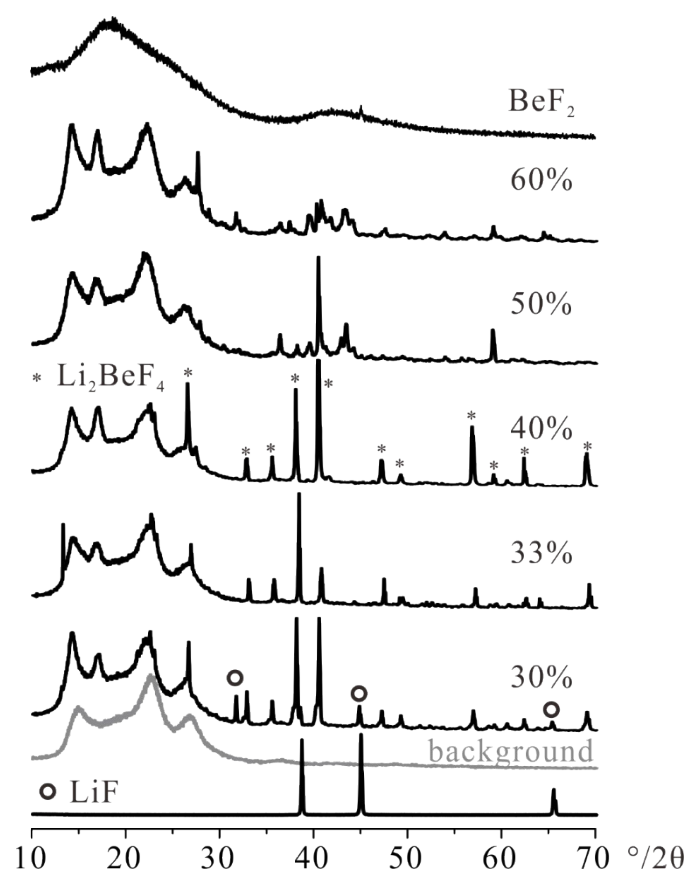


Figure S4. Solid-state ^7Li MAS NMR spectra of FLiBe eutectic salts with different BeF_2 concentration.

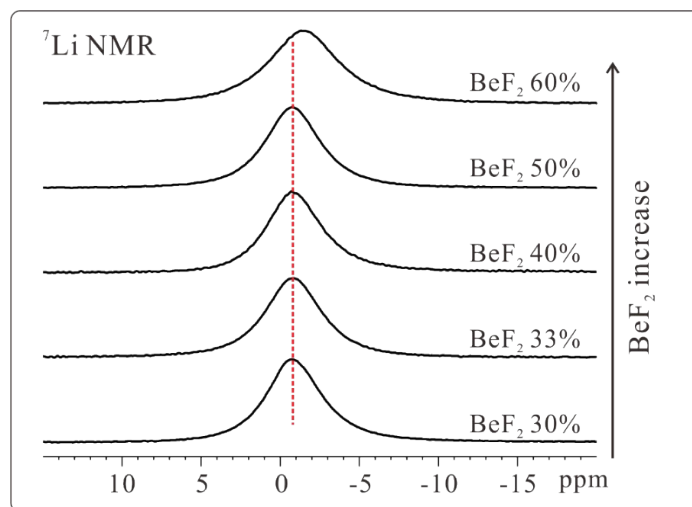
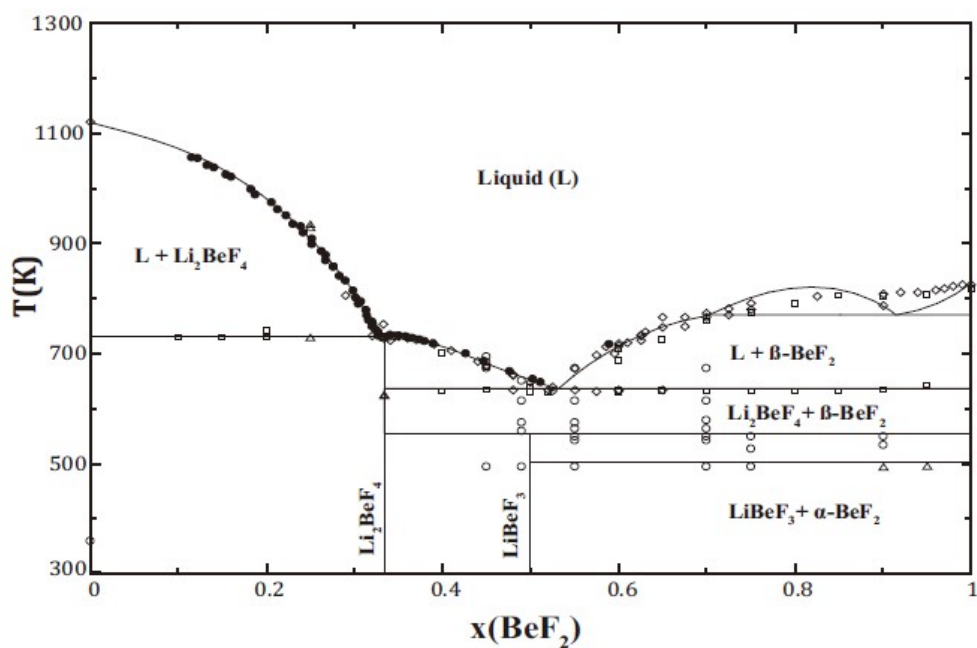
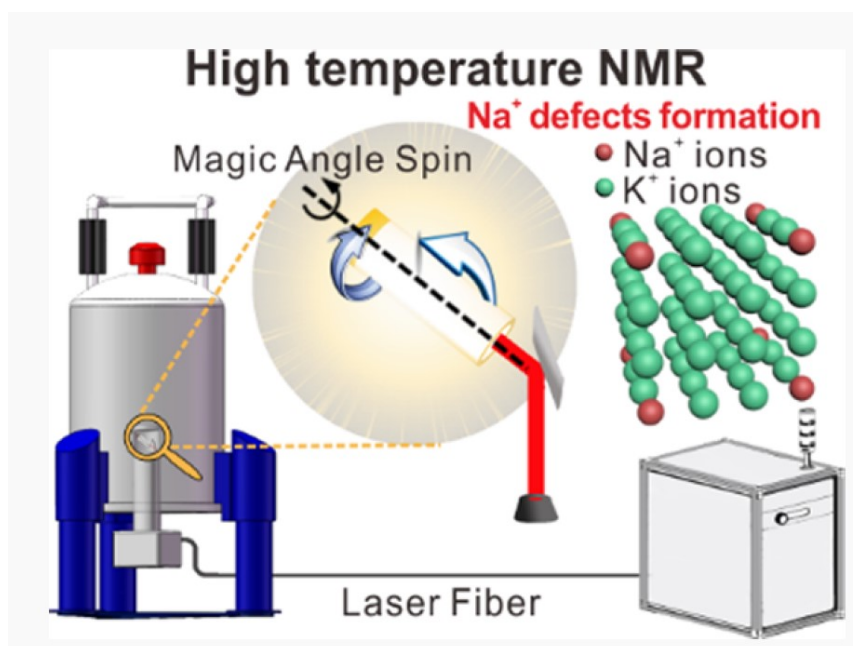


Figure S5. Calculated LiF-BeF₂ phase diagram. (J. Mol. Liq. 299, 112165 (2020).)



1, Smith, A. L., Capelli, E., Konings, R. J. M. & Gheribi, A. E. A new approach for coupled modelling of the structural and thermo-physical properties of molten salts. Case of a polymeric liquid LiF-BeF₂. J. Mol. Liq. 299, 112165 (2020).

Figure S6. Illustration of the laser-heating high-temperature NMR system. Adapted from ref. 2 with permission from the American Chemical Society, Copyright 2021. (*J. Phys. Chem. C* **125**, 4704–4709 (2021))



2, Liu, Y. et al. High-Temperature Magic-Angle Spin Nuclear Magnetic Resonance Reveals Sodium Ion-Doped Crystal-Phase Formation in FLiNaK Eutectic Salt Solidification. *J. Phys. Chem. C* **125**, 4704–4709 (2021).

Figure S7. High-temperature ^{19}F NMR signal simulations and the calculated average chemical shifts.

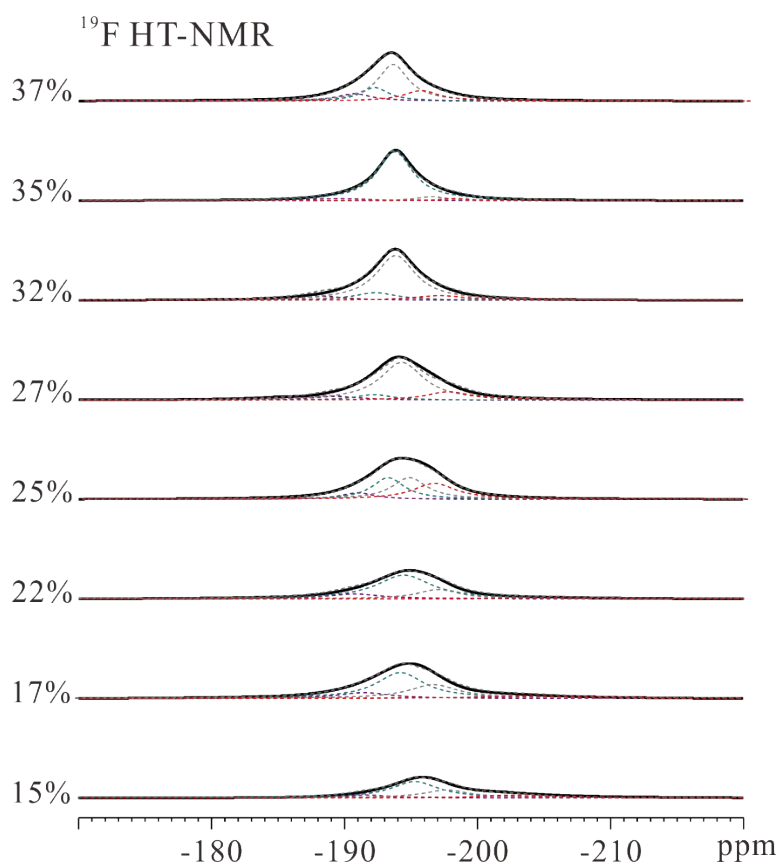


Table S1. Simulated ^{19}F NMR signal chemical shifts.

BeF ₂ concentration	Sig. 1	Sig. 2	Sig.3	Sig.4
15	-192.42	-195.37	-197.28	-201.01
17	-192.3	-194.47	-196.46	-202.12
22	-191.5	-194.49	-196.55	-204.07
25	-191.53	-193.38	-194.67	-196.21
27	-190.53	-192.45	-193.83	-196.17
32	-190.09	-192.66	-193.65	-195.82
35	-191.09	-193.74	-195.46	-196.62
37	-191.06	-192.3	-193.42	-195.14

Table S2. Simulated ^{19}F NMR signal integrals.

BeF ₂ concentration	Sig. 1	Sig. 2	Sig.3	Sig.4
15	0.0879	0.5549	0.2595	0.0977
17	0.1198	0.5085	0.2797	0.092
22	0.1296	0.6435	0.192	0.0349
25	0.0907	0.2966	0.3207	0.292
27	0.082	0.0874	0.6736	0.157
32	0.0674	0.128	0.7132	0.0915
35	0.0595	0.855	0.0577	0.0277
37	0.1208	0.1769	0.5271	0.1751

Table S3. Calculated ^{19}F NMR signal averaged chemical shifts.

BeF ₂ concentration	Averaged chemical shift
15	-196.157
17	-195.47
22	-194.832
25	-194.452
27	-193.806
32	-193.501
35	-193.742
37	-193.219

To obtain the chemical shifts accurately, signal simulation was performed on the ^{19}F HT-NMR signals. The signal simulations were carried out by Dmfit.³ The simulated chemical shifts and integrals were list in Table S1 and S2. The averaged chemical shift was calculated by the equation below:

$$\text{average chemical shift} = (\text{Sig. 1 integral}) * (\text{Sig. 1 chemical shift}) + (\text{Sig. 2 integral}) * (\text{Sig. 2 chemical shift}) + (\text{Sig. 3 integral}) * (\text{Sig. 3 chemical shift}) + (\text{Sig. 4 integral}) * (\text{Sig. 4 chemical shift})$$

The calculated chemical shifts were listed in Table S3.

3, D. Massiot, F. Fayon, M. Capron, et al., Modeling one and two-dimensional solid-state NMR spectra, *Magn. Reson. Chem.* **40** 70–76 (2002).

Figure S8. High-temperature ^9Be NMR signal simulations and the calculated average chemical shifts.

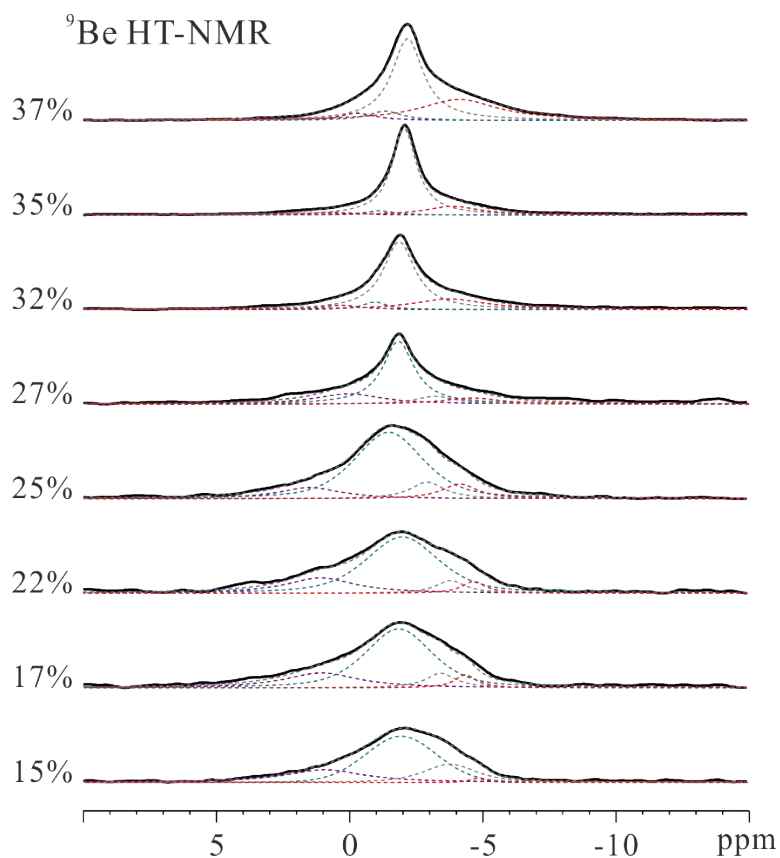


Table S4. Simulated ^9Be NMR signal chemical shifts.

BeF ₂ concentration	Sig. 1	Sig. 2	Sig.3	Sig.4
15	0.9	-1.97	-3.81	-4.85
17	1.03	-1.9	-3.51	-4.44
22	1.16	-1.91	-3.73	-4.6
25	1.42	-1.57	-3.02	-4.25
27	0.04	-1.85	-3.24	-4.63
32	0.3	-0.99	-1.91	-3.81
35	0.66	-1.13	-2.09	-3.93
37	-0.25	-1.31	-2.16	-4.09

Table S5. Simulated ^9Be NMR signal integrals.

BeF_2 concentration	Sig. 1	Sig. 2	Sig.3	Sig.4
15	0.2394	0.5495	0.1975	0.0135
17	0.2173	0.6403	0.0869	0.0555
22	0.2087	0.6634	0.073	0.0549
25	0.1272	0.6757	0.1019	0.0952
27	0.2049	0.5922	0.0958	0.1071
32	0.0499	0.0553	0.6593	0.2355
35	0.0431	0.0435	0.7488	0.1645
37	0.0526	0.0649	0.5399	0.3425

Table S6. Calculated ^9Be NMR signal averaged chemical shifts.

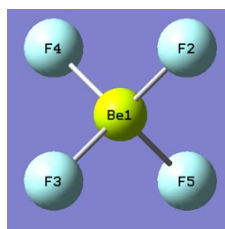
BeF_2 concentration	Averaged chemical shift
15	-1.68501
17	-1.54419
22	-1.54983
25	-1.59256
27	-1.89364
32	-2.1963
35	-2.23219
37	-2.66518

The averaged ^9Be chemical shift was also calculated using same method as ^{19}F NMR signal.

Figure S9. DFT calculation results of ^{19}F and ^9Be NMR chemical shifts of different Be-F species.

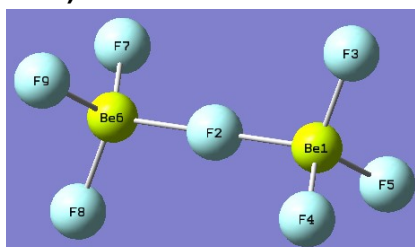
Method: B3LYP/AVTZ

BeF_4^{2-} (Group Point : TD)



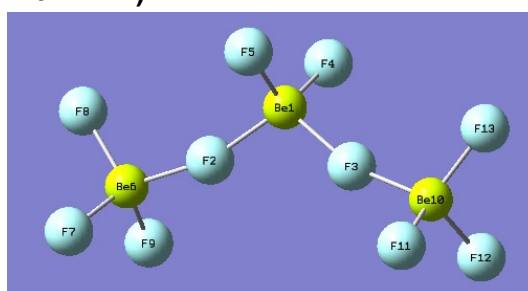
Elem	Atoms	Chemical shift (ppm)	Degeneracy
Be	1	-1.9184	1
F	2,3,4,5	-197.4373	4

$\text{Be}_2\text{F}_7^{3-}$ (Group Point : D3D)



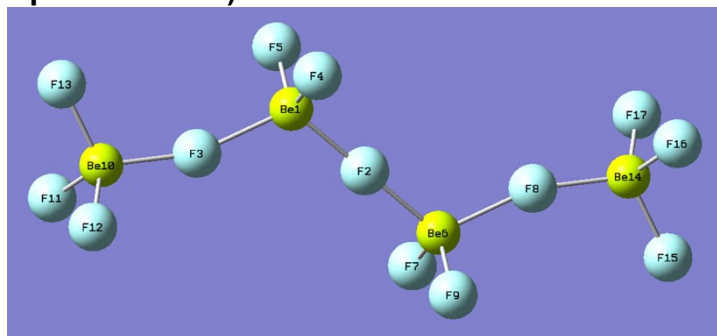
Elem	Atoms	Chemical shift (ppm)	Degeneracy
Be	1,6	-2.2788	2
F	2	-175.407	1
F	3,8,4,5,7,9	-194.87	6
F average		-192.089	7

$\text{Be}_3\text{F}_{10}^{4-}$ (Group Point : C2V)



Elem	Atoms	Chemical shift (ppm)	Degeneracy
Be	6,10	-2.2938	2
Be	1	-2.5235	1
F	2,3	-175.761	2
F	4,5	-191.471	2
F	7,9,11,12	-193.214	4
F	8,13	-195.101	2
Be average		-2.3704	3
F average		-189.752	10

Be₄F₁₃⁵⁻ (Group Point : C_{2h})



Elem	Atoms	Shielding (ppm)	Degeneracy
Be	10,14,1,6	-2.3769	4
F	2	-172.773	1
F	3,8	-177.843	2
F	4,5,7,9	-188.842	4
F	11,12,16,17	-191.737	4
F	13,15	-194.619	2
F average		-187.693	13

Figure S10. Calculated ^{19}F and ^9Be NMR chemical shift evolution plots.

